Phonon-Assisted Indirect Transitions in Cadmium Sulfate Crystals

C. S. Sunandana *
Materials Science Research Centre, Indian Institute of Technology, Madras 600 036 (India)

and

C. Ramasastry
Department of Physics, Indian Institute of Technology, Madras 600 036 (India)

Z. Naturforsch. **33a**, 815—821 (1978); received January 26, 1978

The fundamental absorption edge of "suprapur" cadmium sulphate ($3\,CdSO_4 \cdot 8\,H_2O$) crystal occurs in the region below 200 nm. The power-law dependence of the optical density on photon energy suggests indirect electronic transitions made possible by the emission or absorption of 0.067 eV phonons. The indirect band gap (E_g') at 300 K is 6.09 eV. The phonon energy of 0.067 eV is found to arise from one of the Raman-active modes (E) of the sulphate ion. The band edge is found to shift monotonically towards higher energies at a rate of -2.3 meV per K between 300 and 77 K. The laser Raman spectrum of the $3\,CdSO_4 \cdot 8\,H_2O$ is also reported.

Introduction

The intrinsic optical absorption by crystals has been treated by Fan [1], Bardeen et al. [2], Dexter [3], and Elliott [4], and expressions have been set up for the absorption coefficients for electronic transitions across the forbidden energy gap as well as for excitonic transitions, on the basis of the spherical energy-band approximation viz. $E_k = \hbar^2 k^2/2m$. These theories have been found specially suitable for application to the optical absorption in semiconductors such as Ge [5], Si [6], GaAs [7], SiC [8], $GaAs_{1-x}P_x$ [9], $GeAs_2$ [10], CdTe and ZnTe (amorphous) [11], CdTe [12], CdF_2 [13], CdI_2 [14], $SiSe_2$ [15], SnSe and SnS [16], as well as in ionic crystals such as silver halides [17—19], $SrTiO_3$ [20], alkali halates ($NaClO_3$, $NaBrO_3$, $KClO_3$ and $NaIO_3$) [21] and Tl_2SO_4 [22].

The analysis of the experimental data involves the examination of the shape of the fundamental absorption edge in regard to the power-law dependence of the absorption constant α (cm^{-1}) as a function of the photon energy, and the shift in the position of the band edge with temperature. Such studies in the above cases established the electronic transitions (direct or phonon-assisted) and led to reasonably accurate values of the direct or indirect band gaps E_g or E_g', their changes with temperature, and the phonon energies (E_p) involved. It is an interesting result that not only low-energy lattice modes but also the internal vibrations of the molecular ion groups ClO_3^- and SO_4^{--} can take part in the indirect transitions.

This paper reports the results of optical absorption measurements on single crystals of cadmium sulphate ($3\,CdSO_4 \cdot 8\,H_2O$) and their analysis in the framework of indirect band-to-band transitions. The laser Raman spectra of these crystals are also presented.

Experimental

$3\,CdSO_4 \cdot 8\,H_2O$ crystals were grown by slow evaporation of aqueous solutions of "AnalaR" (BDH), "GR" (S. Merck Co.), "pro analysi" (EMA) and "suprapur" (EMS) (both of E. Merck) materials, at 25 °C. Transparent single crystals with well-developed morphological features were obtained. The flat face is [001] for this monoclinic crystal. The optical absorption spectra were recorded on a Cary-14 double-beam spectrophotometer, while the Raman spectra were recorded on a Coderg laser Raman spectrometer which employs a "Spectra-Physics 125" He-Ne laser with an output power of 50 mW and excitation wavelength 6328 Å. The Cary instrument was continuously flushed with dry nitrogen gas while recording spectra below 195 nm.

Results and Discussion

Figure 1 shows the optical absorption spectra of three EMS cadmium sulphate crystals at 300 K. The crystals are transparent right upto 210 nm, and below that wavelength the absorption rises —

---

* To whom Reprint requests are to be sent.

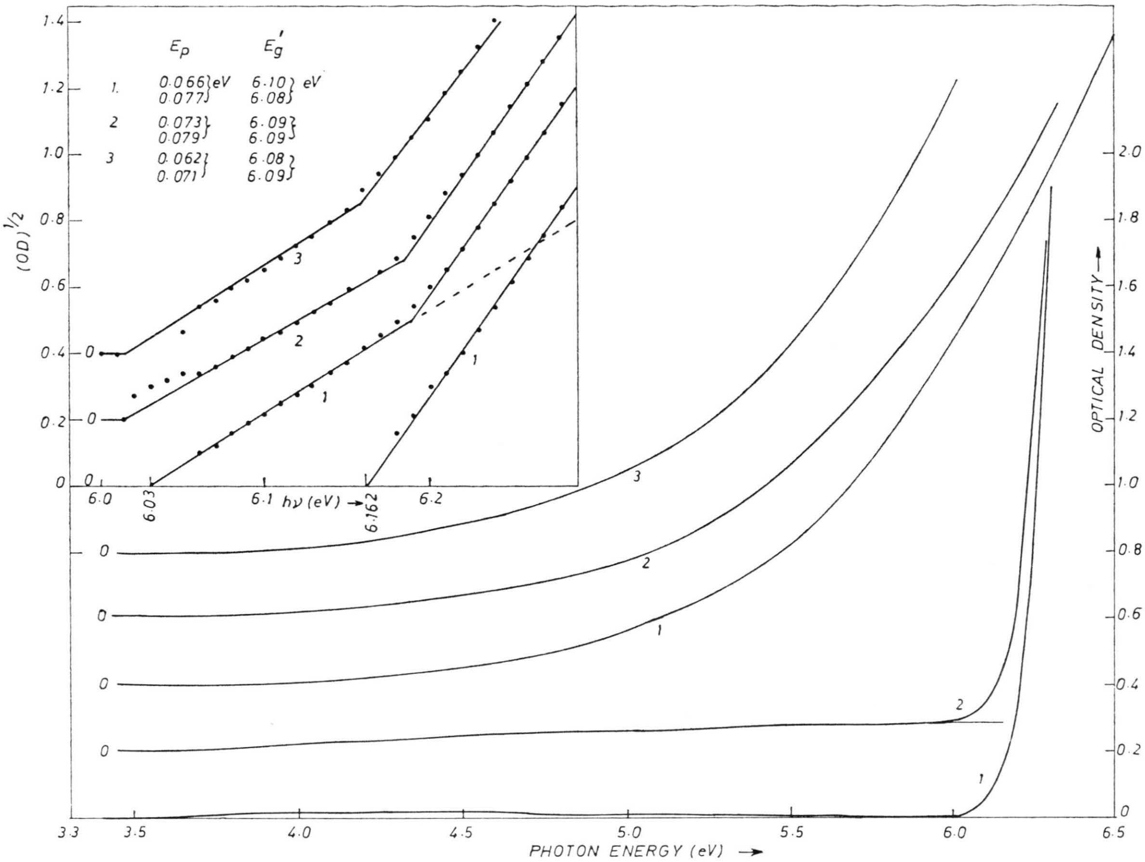

Fig. 1. Optical absorption spectra of three suprapur $3CdSO_4 \cdot 8H_2O$ crystals at 300 K; curve 1 is for a grown crystal (EMS-1) while curve 2 is for a crystal which is found in the original packing of the starting material itself (EMS-0). The data of curve 2 are replotted above to an expanded scale after subtracting a constant background optical density (shown by the extrapolated straight line). Also shown are replotted curve 1 for EMS-1 and curve 3 for EMS-3. The inset shows $(OD)^{1/2}$ vs. $h\nu$ plots for the three crystals, representing the phonon absorption and emission parts. For 1, the emission part is separately plotted after subtracting the extrapolated absorption part from the total absorption. The threshold energies are indicated. They are practically the same for the three crystals. The two sets of E_p and E_g' listed for the three crystals were obtained by taking the threshold $h\nu_e$ as (i) the $h\nu$ where α_{abs} is practically zero, and (ii) the $h\nu$ where the two straight lines intersect.

gradually at first and then steeply — reaching absorption coefficients of the order of 50 cm^{-1} at 190 nm, which is the wavelength limit of the spectrophotometer. However, in some cases (for example, curve 2) there is background absorption due to reflections and scattering, and this could be corrected for, at least approximately, by extrapolating the linearly increasing absorption from the long wavelength end and subtracting the extrapolated optical density (OD) from that of the absorption edge. The corrected OD's are plotted to a bigger scale in the same Figure 1. It is to be mentioned that OD's below 0.05 could be in error by as much as 30—50% and the square roots of the OD's would exaggerate this errror even more. This fact should be borne in mind in analysing the long-wavelength tail.

Figure 2 shows the temperature dependence of the absorption edge of one of the EMS crystals. On cooling the crystal from 300 K to 109 K, the band edge shifts monotonically towards higher energies. The magnitude of the absorption coefficient (~ 50 cm^{-1}) as well as the temperature-dependence of the absorption edge suggest that we are dealing here with the intrinsic optical band edge absorption of the crystal.

To decide about the nature of the transition — direct or indirect, allowed or forbidden, band-to-band or excitonic — various power-law dependences of the observed OD: $(OD)^{1/2}$, $(OD)^{2/3}$, $(OD)^2$ and

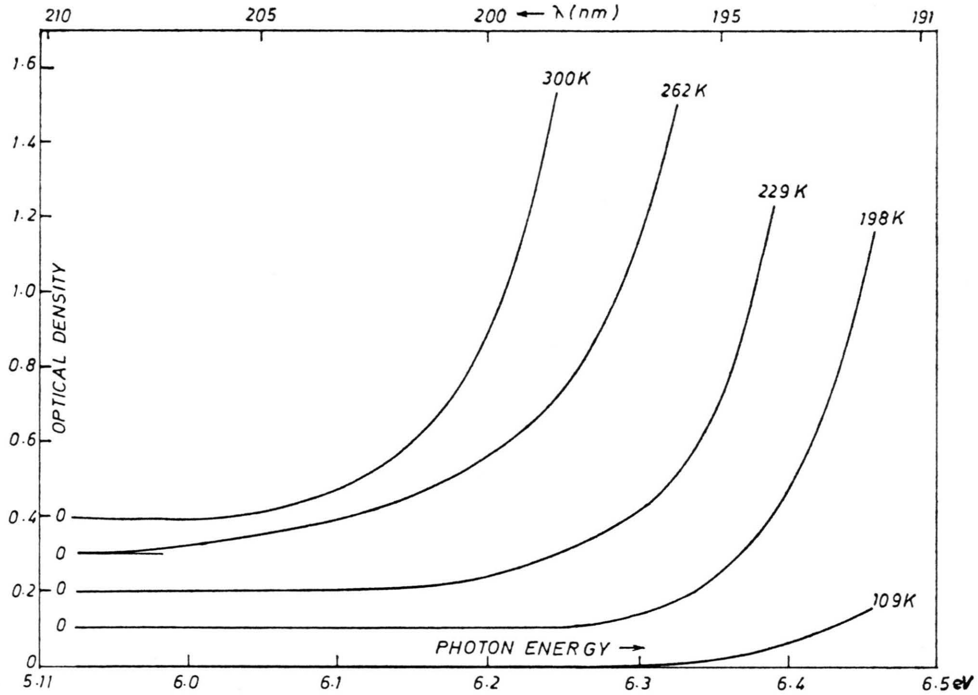

Fig. 2. Temperature dependence of the optical absorption of "suprapur" $3CdSO_4 \cdot 8H_2O$ (EMS-3). The edge shifts monotonically to higher energies on cooling the crystal from 300 to 109 K. At 109 K only a small portion of the tail of the band edge is seen. Also there is an abrupt decrease in the optical density in going from 198 K to 109 K, which might be associated with a phase transition in the crystal.

log OD, on photon energy were examined [22]. It was found that a plot of $(OD)^{1/2}$ versus $h\nu$ gave two straight lines (Inset, Figure 1). It should be mentioned that the Urbach formula was found to fit the central region of the absorption edge — in the range 6.15—6.275 eV the log OD vs. $h\nu$ plot is linear — but considerable deviations occurred in the tail as well as the steeper regions of the edge. Thus the observed absorption of $3CdSO_4 \cdot 8H_2O$ could be interpreted as arising from indirect band-to-band electronic transitions assisted by phonons which consists of two contributions — one due to phonon emission and the other due to phonon absorption:

$$\alpha = \alpha_{em} + \alpha_{abs} = \frac{a(h\nu - E_g' - E_p)^2}{1 - \exp(-E_p/kT)} + \frac{b(h\nu - E_g' + E_p)^2}{\exp(E_p/kT) - 1}, \qquad (1)$$

where E_g' and E_p are the indirect band gap energy and phonon energy respectively, and a and b are constants involving the square of the matrix elements for the probability of the electronic transitions with phonon emission and absorption, respectively. The denominators of Eq. (1) arise from the introduction of phonon occupation numbers in Bose-Einstein statistics. The threshold energies for phonon emission and absorption (as determined from a plot of $(OD)^{1/2}$ vs. $h\nu$) are given by

$$h\nu_e = E_g' + E_p,$$
$$h\nu_a = E_g' - E_p, \qquad (2)$$

from which E_g' and E_p could be evaluated. From an analysis of the data on several crystals, a value 6.09 ± 0.01 eV for E_g' at 300 K and a value 0.067 ± 0.005 eV for E_p were obtained in the case of $3CdSO_4 \cdot 8H_2O$. Table 1 gives the absorption edge data on some halate and sulphate crystals, all reported from this laboratory.

In the inset of Fig. 1, the phonon absorption and emission parts are separated out for one of the crystals (EMS-1), by extrapolating the phonon absorption part to higher energies and subtracting the extrapolated OD from the total OD and replotting. As the "knee" is not sharp in going from phonon absorption to phonon emission part,

Table 1. Absorption Edge Data on Some Halate and Sulphate Crystals.

Crystal	E_g' (eV)	E_p (eV)	$\partial E_g'/\partial T$ (eV per °K)	Reference
$NaClO_3$	5.311[a]	0.23 ± 0.02 0.065 ± 0.01	-3.75×10^{-4}	21
$KClO_3$	5.398[a]	0.23 ± 0.02 0.065 ± 0.01	-5.0×10^{-4}	21
$NaBrO_3$	4.365[a]	0.18 ± 0.02 0.055 ± 0.01	-2.5×10^{-4}	21
$NaIO_3$	4.115[a]	0.15 ± 0.02	-2.9×10^{-4}	21
Tl_2SO_4	4.5 ± 0.1[b]	0.07 ± 0.01	-2.9×10^{-3}	22
$3CdSO_4 \cdot 8H_2O$	6.09 ± 0.01[b]	0.067 ± 0.005	-2.3×10^{-3}	Present work

[a] At 305 K, [b] at 300 K.

the threshold $h\nu_e$ is taken to be the point at which the OD due to phonon emission is actually zero. The two sets of E_g' and E_p values listed in the inset correspond to $h\nu_e$ being taken at $(OD)_{em} = 0$ and at the pont of intersection of the two straight lines, respectively.

Incidentally, the value of E_p viz. 0.067 ± 0.005 eV, agrees rather well with that obtained for Tl_2SO_4 [22] i.e. 0.07 eV. This probably means that — as in the case of $NaClO_3$ and $KClO_3$ [21] which have given absorption edges due to indirect electronic transitions assisted by ClO_3^- ion vibrations — the common SO_4^{--} vibrations are involved in the electronic transitions in Tl_2SO_4 and $3CdSO_4 \cdot 8H_2O$.

$(OD)^{1/2}$ vs. $h\nu$ plots for the different low-temperature curves of Fig. 2 also yield two straight-lines with nearly equal intercepts ($2E_p$). The slope of the α_{em} part does not change appreciably with temperature, as expected. Below 198 K, there appears to be an abrupt fall in absorption, probably because of a phase change. At 109 K, the edge has shifted so much into the far ultraviolet that the emission part is nearly absent in our record. The edge shifts at the rate of -2.3 meV per degree K, in the temperature range 300 K to 200 K.

Further, the data at 109 K could not be analysed because the low OD values are in error due to stray light effects, scattering and quartz window absorption. The spectra should be recorded at still lower temperatures, preferably down to 4 K, in a vacuum ultra-violet instrument in order to check if the phonon absorption part of the curve disappears for such low temperatures at which the phonon population is very small. Going down to 4 K with our quartz instrument would not help because the absorption edge would have shifted still further to shorter wavelengths.

Figure 3 shows the optical absorption spectra of "AnalaR" (BDH), GR, EMA and EMS cadmium sulphate crystals at 300 K. Except EMS crystal, which exhibits only the absorption edge, all other crystals show at least three absorption bands (A, C and D). Gaussian analysis of the bands is given in the case of curve b, in which case a maximum of four peaks occurred. Table 2 lists the peak positions and half-widths of the absorption bands. These bands might be due to one or more of the trace impurities present in the relatively impure starting materials (except "suprapur"). As the peak positions of the A and C bands are nearly the same in BDH and GR crystals and their heights are in the ratio 1:3, they might be due to a single common impurity. However, the EMA crystals show two close-lying bands of comparable intensity (A and C). Cooling the crystals to 77 K did not result in any appreciable resolution of the bands (cuve a_1 of Fig. 3), especially in the tail region of the band edge, thus making isolation of the bands difficult. X-irradiation and doping with manganese did not help characterise the impurity. In such circumstances, it is suggested that copper and/or lead ions, present in their diamagnetic states, might be responsible for the observed absorption bands, as these two metal ions are listed by the manufacturers in the assay. More systematic work is needed to identify the impurity.

Figure 4 shows the laser Raman spectrum of cadmium sulphate single crystal at 300 K. There are three bands at 460, 999 and 1098 cm^{-1} (which correspond to 0.057, 0.124 and 0.136 eV) with relative intensities of 6:21:3. These bands could be assigned to the bending (E), totally symmetric (A_1) and asymmetric stretch (T_2) modes of the SO_4^{--} ion (cf. ref. [23]). No lattice modes could be seen.

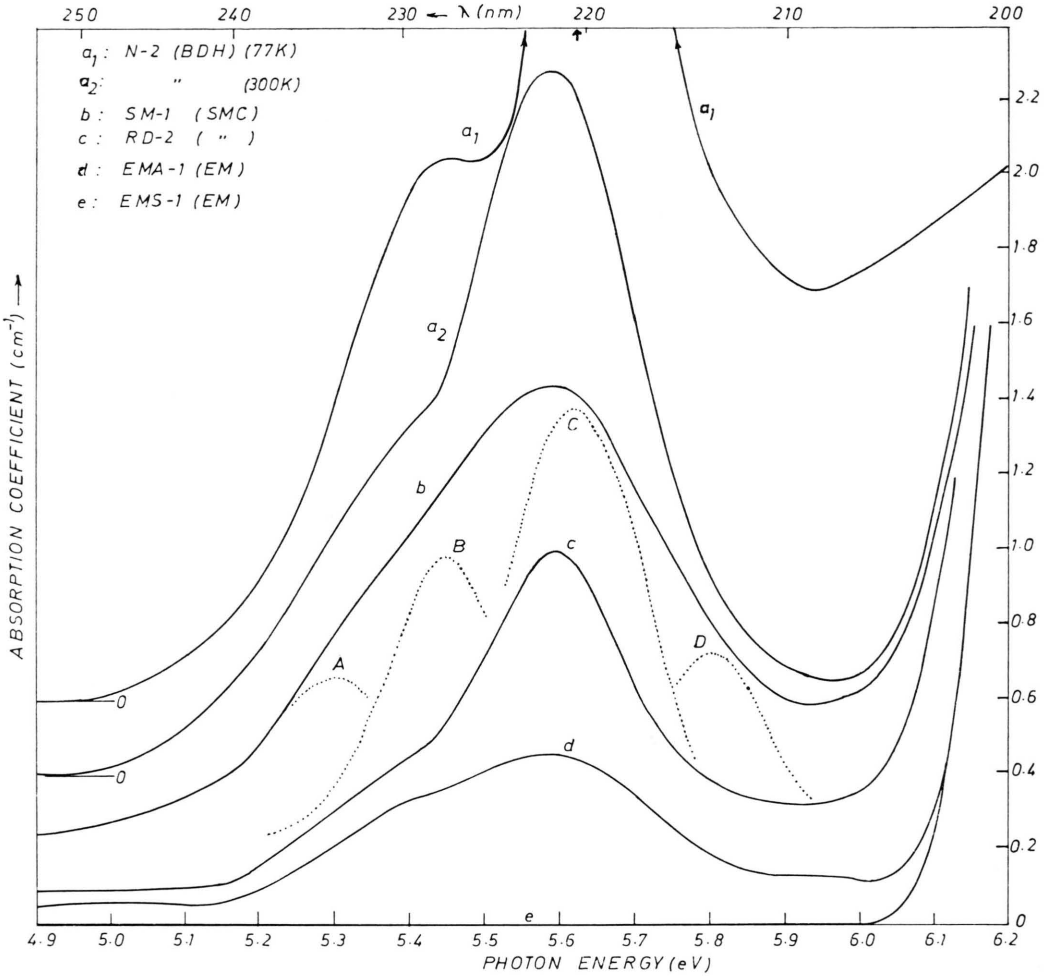

Fig. 3. Optical absorption spectra of $3CdSO_4 \cdot 8H_2O$ crystals grown from four source materials: "AnalaR" (BDH) at 77 K and 300 K (curves a_1 and a_2), "GR" (S. Merck) (curves b and c), "pro analysi" (E. Merck) (curve d), and "suprapur" (E. Merck) (curve e), all at 300 K. Curves a_1 — d are analysed into Gaussian absorption bands (peak positions and half-widths are listed in Table 2). A maximum of four (A, B, C and D) bands are observed in the case of curve b. From the nearly equal ratio of heights (1:3) of the A and C peaks in the case of curves a_2, b and c, it is inferred that these bands arise from a single, common impurity. Resolution at 77 K, in the tail portion of the band edge, is not sufficient (curve a_1) to separate out the bands present in that region.

Table 2. Gaussian Analysis ($D = D_0 \exp[\{-4 \ln 2/(W_{1/2})^2\}(E - E_0)^2]$) of impurity absorption Bands in $3CdSO_4 \cdot 8H_2O$ Crystals at 300 K.

Crystal Code	Purity	Peak A			Peak B			Peak C			Peak D			Ref. to Fig. 3
		E_0 (eV)	$W_{1/2}$ (eV)	D_0	E_0 (eV)	$W_{1/2}$ (eV)	D_0	E_0 (eV)	$W_{1/2}$ (eV)	D_0	E_0 (eV)	$W_{1/2}$ (eV)	D_0	
N-2	"AnalaR" (BDH)	5.30	0.58	0.58				5.59	0.27	1.86				curve a_2
SM-1	"GR" (S. Merck)	5.30	0.19	0.27	5.45	0.20	0.49	5.62	0.21	0.75	5.80	0.21	0.31	curve b
RD-2	"GR" (S. Merck)	5.38	0.23	0.26				5.60	0.22	0.88	5.86	0.25	0.22	curve c
EMA-1	"pro analysi" (E. Merck)	5.40	0.25	0.24				5.62	0.25	0.38				curve d

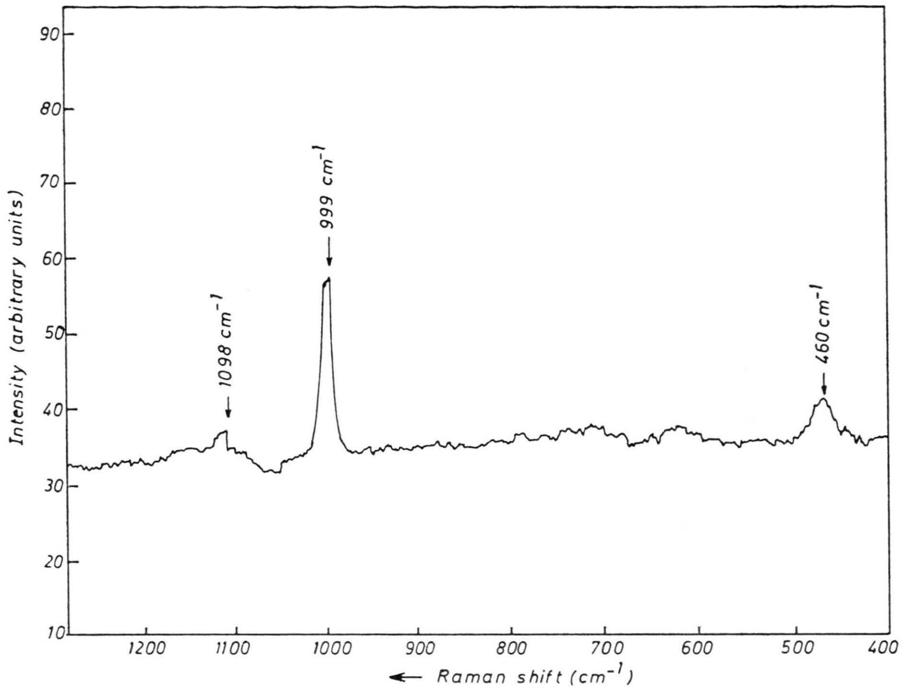

Fig. 4. Laser Raman spectrum of cadmium sulphate single crystal at 300 K. The three peaks at 460, 999 and 1098 cm^{-1} are attributed to the three internal modes E, A_1 and T_2, of the sulphate ion. No lattice modes are observed.

The Boltzmann factors $[\exp(-E_p/kT)]$ at 300, 100 and 77 K, corresponding to E_p values of 0.057, 0.124 and 0.136 eV (internal mode energies of SO_4^{--}) are given in Table 3. There will be enough population of 0.057 eV phonons even at 77 K so that phonon absorption is possible at 77 K, though with considerably reduced intensity. The situation is similar to that of ClO_3^- ion in $NaClO_3$ [21] where is was found that 0.065 eV phonons did not decay even at 77 K while the 0.23 eV phonons disappeared as early as 153 K (the $(OD)^{1/2}$ vs. $h\nu$ plot gave only three straight lines at this temperature). In the present case it could be that the E_p of 0.067 eV represents the energy of the bending mode of SO_4^{--} ions, namely 0.057 eV, the deficit of 0.01 eV being accountable by a lattice phonon of requisite energy which will be available down to very low temperatures. As mentioned earlier, a study in vacuum ultraviolet at temperatures below 77 K is needed to decide between the several alternatives. Such a study is, at present, beyond our experimental means.

In conclusion, therefore, the intrinsic optical absorption in cadmium sulphate crystals arises from indirect band-to-band electronic transitions in which the sulphate ion vibration 0.057 eV takes part.

Table 3. Boltzmann factors $(\exp(-E_p/kT))$ for Raman-active modes of SO_4^{--} in $3CdSO_4 \cdot 8H_2O$.

Temperature (K)	$\exp(-E_p/kT)$ for		
	$E_p = 0.057$ eV (E mode)	$E_p = 0.124$ eV (A_1 mode)	$E_p = 0.136$ eV (T_2 mode)
300	1.1×10^{-1}	8.5×10^{-3}	5.3×10^{-3}
100	2.2×10^{-4}	5.6×10^{-7}	1.4×10^{-7}
77	1.8×10^{-4}	6.8×10^{-9}	1.0×10^{-9}

[1] H. Y. Fan, Repts. Prog. Phys. **19**, 107 (1956).
[2] J. Bardeen et al. Photoconductivity Conference, Eds. R. G. Breckenridge et al., Wiley, New York 1954.
[3] D. L. Dexter, ibid.
[4] R. J. Elliott, Phys. Rev. **108**, 1384 (1957).
[5] G. G. Macfarlane et al., Phys. Rev. **108**, 1377 (1957).
[6] G. G. Macfarlane et al., Phys. Rev. **111**, 1245 (1958).
[7] T. S. Moss, J. Appl. Phys. **32** (Suppl.), 2136 (1961).
[8] W. J. Choyke and Lyle Patrick, Phys. Rev. **187**, 1041 (1969).
[9] A. N. Pikhtin et al., Phys. Stat. Sol. (b) **50**, 717 (1972).
[10] J. W. Rau and C. R. Kannewurf, Phys. Rev. **B 3**, 2581 (1971).
[11] H. M. Brown and D. E. Brodie, Can. J. Phys. **50**, 2502 (1972).
[12] D. T. E. Morple, Phys. Rev. **150**, 728 (1966).
[13] R. A. Forman et al., Solid state commun. **10**, 19 (1972).
[14] Ya. O. Dovgiy et al., Ukrainian J. Phys. (USA) (1970); P. A. Lee et al., J. Phys. Chem. Solids **30**, 2719 (1969).
[15] E. A. Hauschild and C. R. Kannewurf, J. Phys. Chem. Solids **30**, 353 (1969).
[16] K. Takahashi et al., Science of Light (Tokyo), **21**, 131 (1972).
[17] F. C. Brown et al., J. Phys. Chem. Solids **22**, 101 (1961).
[18] B. L. Joesten and F. C. Brown, Phys. Rev. **148**, 919 (1966).
[19] A. P. Marchetti and G. L. Bottger, Phys. Rev. **B 3**, 2604 (1971).
[20] M. Capizzi and A. Frova, Phys. Rev. Lett. **25**, 1298 (1970).
[21] S. B. S. Sastry, R. B. Tripathi, and C. Ramasastry, J. Nonmetals **1**, 93 (1972); J. Phys. Chem. Sol. **34**, 473, 481 (1973).
[22] C. Ramasastry, C. S. Sunandana, and B. S. V. S. R. Acharyulu, J. Nonmetals **1**, 283 (1973).
[23] R. E. Hester and R. A. Plane, Inorg. Chem. **3**, 769 (1969).